

Assessment of Reaction-Rate Predictions of a Collision-Energy Approach for Chemical Reactions in Atmospheric Flows

M. A. Gallis¹, R. B. Bond², J. R. Torczynski³

Sandia National Laboratories,

Albuquerque, New Mexico 87185-0346 USA

A recently proposed approach for the Direct Simulation Monte Carlo (DSMC) method to calculate chemical-reaction rates is assessed for high-temperature atmospheric species. The new DSMC model reproduces measured equilibrium reaction rates without using any macroscopic reaction-rate information. Since it uses only molecular properties, the new model is inherently able to predict reaction rates for arbitrary non-equilibrium conditions. DSMC non-equilibrium reaction rates are compared to Park's phenomenological non-equilibrium reaction-rate model, the predominant model for hypersonic-flow-field calculations. For near-equilibrium conditions, Park's model is in good agreement with the DSMC-calculated reaction rates. For far-from-equilibrium conditions, corresponding to a typical shock layer, significant differences can be found. The DSMC predictions are also found to be in very good agreement with measured and calculated non-equilibrium reaction rates, offering strong evidence that this is a viable and reliable technique to predict chemical reaction rates.

Nomenclature

b	scattering parameter	(pure)
c_r	relative speed	(m/s)
C_1, C_2	cross section parameters	(pure)
E_t	translational energy	(J)
E_i	internal energy	(J)
$E_c = E_t + E_i$	collision energy	(J)
i	vibrational energy state	(pure)
$K_{eq,r}$	equilibrium reaction constant	(pure)
k	reaction rate	($\text{m}^3 \text{molecule}^{-1} \text{s}^{-1}$)
k_B	Boltzmann constant	(J/K)
m	mass	(kg)
q	temperature exponent in Park's model	(pure)
r	distance	(m)
T	temperature	(K)
z_v	vibrational partition function	(pure)
Z_i	vibrational relaxation number	(pure)
Z	non-equilibrium reaction rate parameter	(pure)

Greek

α	VSS angular scattering parameter	(pure)
Γ	gamma function	(pure)
ε_i	specific internal energy of mode i	(J kg^{-1})

¹ Principal Member of Technical Staff, Microscale Sciences and Technology Department, MS 0346, Senior AIAA Member.

² Senior Member of Technical Staff, Aerosciences Department, MS0836, Member AIAA.

³ Distinguished Member of Technical Staff, Microscale Sciences and Technology Department, MS 0346.

ε	symmetry parameter	(pure)
ζ	degrees of freedom	(pure)
Θ_d	characteristic dissociation temperature	(K)
	characteristic vibrational temperature	(K)
Λ	reaction rate constant	(pure)
μ	viscosity	(Nsm ⁻²)
ν	IPL distance exponent	(pure)
σ	cross section	(m ²)
ϕ	fraction of collisions exchanging internal energy	(pure)
χ	scattering angle	(deg)
ω	viscosity temperature exponent	(pure)

Acronyms

ADM	Adiabatic Dissociation Model
CCI	Contracted Configuration Interaction
CE	Chapman-Enskog
CVD	Chemical Vapor Deposition
DSMC	Direct Simulation Monte Carlo
GLB	General Larsen-Borgnakke
IPL	Inverse Power Law
ME	Maximum Entropy
M-F	Macheret and Fridman
M-T	Marrone and Treanor
PVD	Physical Vapor Deposition
QCT	Quasi-Classical Trajectory
TCE	Total Collision Energy
VHS	Variable Hard Sphere
VSS	Variable Soft Sphere

Subscripts

a	activation
b	backward
c	collision
d	dissociation
eq	equilibrium
i	internal energy mode
max	maximum
mol	molecule
R	reaction
r	reduced for mass, relative for speed
ref	reference
rot	rotational
t	total
tr	translational
vib	vibrational
1	first order
∞	infinite order

I. Introduction

There is an ever growing number of technologically important areas in gas dynamics such as hypersonic reentry, materials processing and micro-systems for which the gas is not in thermal equilibrium and cannot be characterized by a single temperature. In cases where non-equilibrium gas flows include chemical processes, these occur in an environment very different from the thermal equilibrium environments in which traditional chemical processes take place. For processes in thermal non-equilibrium, established chemistry models, based on the equilibrium Arrhenius rates $k(T)$, cannot be used since the concept of describing the flow using a single temperature T is no longer valid.

The challenges of modeling chemical reactions in a non-equilibrium environment can be exemplified by the case of hypersonic reentry into the earth's atmosphere^{1,2,3} and other planetary atmospheres.⁴ Modeling chemical and ionization reactions at the extreme conditions of hypersonic flow in the upper atmosphere has been a very important problem since the first Apollo-era space flights. However, even today this problem evades a satisfactory solution. The root cause for the inadequate state of modeling is the difficulty in obtaining reliable, internal-energy-state-specific, experimentally measured cross sections for atmospheric species reactions that can be used to validate theoretical models. Efforts by Park,^{2,5} Gupta et al.⁶, and Bortner⁷ to compile a set of chemical reaction rates that could be used for hypersonic applications were hampered by this lack of measurements.

It is indicative of the scarcity and inadequacy of the measurements, even under conditions of thermodynamic equilibrium, that for the so-called, first Zeldovich reaction, $N_2 + O \rightarrow NO + N$, one of the most important reactions in hypersonic flow fields and one of the reactions considered best known, measurements exist only in the regime between 2,384 K-3,850 K. These conditions are vastly different from the non-equilibrium conditions at temperatures in excess of 15,000 K typically met in hypersonic applications. Given the paucity of measurements, current Arrhenius-type chemical reaction rates^{2,6,7} used for hypersonic flow fields are based at best on extrapolations of measured low-temperature equilibrium rates and at worst on estimations from radiation data. For some of the reactions of interest, no experimental data exist, and the reaction rates are mere estimates based on reactions between other species, after having their rates adjusted to reflect the differences in the equilibrium collision frequency.

The state of knowledge for the rates of atmospheric-species reactions under conditions of thermodynamic non-equilibrium is even less advanced. The behavior of atmospheric chemical reactions under conditions of thermal non-equilibrium has not been systematically investigated, and using equilibrium chemical-reaction data in gas dynamics codes to simulate thermal and chemical non-equilibrium in hypersonic flow fields can lead to unknown and potentially large errors in their predictions. Park,^{2,5} in an attempt to include non-equilibrium effects into the calculation of chemical reaction rates, used information from experimental observations and flight data and conjectured that the available reaction-rate data could be better fitted by an Arrhenius-type two-temperature model. According to Park's model, replacing the gas temperature in the Arrhenius rate by the geometric average of the translational and the vibrational temperature of the gas could sufficiently account for non-equilibrium effects.

Park's model has since been the principal method for dealing with non-equilibrium flows within the framework of the Navier-Stokes equations although the suggested mechanisms employ a considerable degree of empiricism. Further research with Park's model has focused on better estimating the dependence of the reaction rate on the energy content of the molecular energy modes and more specifically on the temperatures characterizing the vibrational and the translation modes. Concerns have been voiced (Gupta et al.,⁶ and references therein), mainly based on quantum mechanical calculations, that the selection of temperatures and the weighting of the temperature by the vibrational temperature may not provide a good representation of the actual conditions. For example, it is believed that excitation of the vibrational mode promotes slow endothermic reactions but influences fast endothermic reactions to a lesser extent.⁸

Physico-chemical approaches to quantify the effect of thermodynamic non-equilibrium on chemical reaction rates led to a number of semi-theoretical or semi-empirical models.⁸ These models, lack the generality of the Park model since they are applicable to a particular type of chemical reactions, and they calculate the non-equilibrium reaction rates $k(T_{tr}, T_{vib}, T_{rot}, T_{el})$ as a deviation from the equilibrium reaction rate $k(T)$ using the form $k(T_{tr}, T_{vib}, T_{rot}, T_{el}) = k(T)Z(T_{tr}, T_{vib}, T_{rot}, T_{el})$, where the subscripts tr, vib, rot, el stand for the translational, vibrational, rotational, and electronic energy modes, respectively. These models are useful tools to theoretically describe and evaluate the importance of various competing mechanisms in promoting a reaction. The disadvantage of these models is that the reaction rates, at best estimated from low-temperature equilibrium data, are being used, making the non-equilibrium reaction-rate predictions highly questionable and of unknown accuracy.

The most widely used method for simulating fluid flows uses the continuum fluid mechanics Navier-Stokes equations, which for continuum near-thermodynamic-equilibrium gas dynamics can be derived from the Boltzmann equation based on the perturbation analysis of Chapman and Enskog.⁹ The Navier-Stokes equations, which are physically well founded for continuum near-equilibrium flows, are the most computationally efficient method for gas dynamics. The problem with simulating chemically reacting flows with the Navier-Stokes equations is that all the available computational models implicitly or explicitly depend on the thermal-equilibrium Arrhenius rates. This limits the applicability of the Navier-Stokes equations to the regime where the particular compilation of Arrhenius rates can be trusted.

Unlike Navier-Stokes codes, which require chemical-reaction-rate models as inputs, molecule-based techniques such as the Direct Simulation Monte Carlo (DSMC) method,¹ which deals with individual molecules and their collisions, can simulate gas flows at a more fundamental level that is closer to reality. The DSMC method is capable of simulating non-equilibrium gas behavior based on kinetic theory that calculates molecular collisions using stochastic rather than deterministic procedures as in Molecular Dynamics. This improves the computational efficiency of DSMC greatly compared to other Monte Carlo and “particle” methods. As a result, Bird’s Direct Simulation Monte Carlo (DSMC) method is used almost universally in rarefied gas dynamics and whenever mean-free-path phenomena are of interest.

Two molecules in an intermolecular collision are unaware of the macroscopic temperature of the gas, and the outcome of their collision is controlled only by their orientation, their energy content and its distribution among the available modes of the colliding pair. Therefore, for a chemical-reaction-rate model to be physically realistic and reliable for non-equilibrium flows, it is of paramount importance that it depends only on molecular-level processes and does not rely on equilibrium or macroscopic information. Within the framework of DSMC, an approach for determining chemical-reaction rates from first principles and fundamental microscopic molecular data has recently been developed¹⁰ that obviates the need for any macroscopic rate information. These molecular processes can be used not only to model highly non-equilibrium chemically reactive flows within the context of DSMC but also to develop chemical-reaction-rate models for near-continuum flows that can be used by Navier-Stokes continuum fluid dynamics codes.

Energy exchanges during molecular collisions and chemical reactions are closely connected. Both Newton’s equation of motion for a classical system and Schrödinger’s equation for a quantum system are unchanged by time reversal. Due to this symmetry under time reversal, the probability of a forward chemical reaction from a particular energy state taking place is equal to the probability of this energy state appearing in the products of the reverse reaction. This concept, termed the principle of *microscopic reversibility* or *reciprocity theorem*, is key to the development of chemical reaction models. The statistical relationship between the rate constants for forward and reverse reactions at equilibrium resulting from microscopic reversibility is known as the principle of *detailed balance*.

II. Modeling of Chemical Reactions with DSMC

Molecular-level modeling is ideally suited to the study of chemically reacting gas flows. As such, DSMC procedures entirely based on microscopic properties of the colliding molecules and completely unaware of the macroscopic conditions of the surrounding gas can provide flow-field predictions under arbitrary conditions of non-equilibrium. DSMC procedures for intermolecular collisions employ a cross section that is a function of the relative translational energy of the colliding molecules.¹ It is through Chapman-Enskog theory that this cross section can be related to the temperature-dependent viscosity of the real gas, a physical quantity that can be readily measured. Thus, it is not necessary to introduce a macroscopic temperature to model the translational mode during molecular collisions.

To model chemical reactions within the context the DSMC method, complete tabulations of the cross sections as a function of the impact parameters and energy states of the molecules are needed. Such information could come from quantum mechanical calculations, supported by experiment. However, very little such information is available, and that limited information applies to only a small number of reactions. The complexity of the situation almost guarantees that there will be no significant increase in the amount of such information available in the foreseeable future.

In the absence of such detailed data, DSMC simulations have to resort to phenomenological models, conceptually similar to those used to model intermolecular interactions, that capture the most essential features of the microscopic mechanisms while maintaining the computational efficiency of DSMC. In a similar fashion to the

molecular models used in DSMC, chemistry models aim to reproduce the main properties of the chemical-reaction processes but in a computationally efficient manner. A necessary, but not sufficient, condition for any chemistry model to be valid is its ability to reproduce the equilibrium reaction rates. More advanced features include linking the energy-exchange process to that of chemical reactions and satisfying the principles of macroscopic reversibility at a microscopic level and detailed balance at the macroscopic level.

A. DSMC Chemistry Models

There are many possible ways that DSMC chemistry models can be categorized. Herein, the DSMC models will be partitioned into two main categories: models that use macroscopic equilibrium rate information to calibrate adjustable parameters, and models that use only microscopic and collision-specific information without resorting to adjustable parameters. The former comprise a very large number of models of varying sophistication and complexity. The latter consist of the work by Bird.^{1,10} DSMC chemistry models have been reviewed and comparatively evaluated on many occasions.^{3, 11, 12}

A necessary condition for any model is to be able to reproduce measured Arrhenius reaction rates. Thus, the first model for chemical reactions in DSMC was proposed by Bird¹³ was based on satisfying this requirement. This model, termed the Total Collision Energy (TCE) model, provides a microscopic reaction model that can reproduce the conventional macroscopic Arrhenius rate equation in the continuum limit. The model, based on considerations of mathematical tractability, is evidently phenomenological in nature. This model has been used extensively in DSMC simulations and produces results that are in good agreement with measurements.¹

The suggestion that particular energy modes may play a more important role in determining the probability of a chemical reaction taking place was central to many other models, some of them extensions of the TCE model, proposed for use in DSMC.^{3,12} A common feature of all these models is the assumption of a particular form of the reaction cross section, a function of the total as well as particular energy modes, and the requirement that these cross sections reproduce a known Arrhenius-type reaction rate. In some cases these models are compared to measured or calculated cross sections. Comparisons of the predictions of the TCE model and its variants for non-equilibrium calculated cross sections for exchange reactions³ indicates that the calculated cross sections are of the correct order, which provides some basis for optimism that the non-equilibrium predictions of the model can be considered reliable within the expected error of the method. However, caution must be exercised since detailed cross-section and rate comparisons by Wysong et al.¹⁴ indicate that extracting adjustable parameters from measured or extrapolated equilibrium reaction rates may lead to unphysical reaction cross sections. Regardless of the ability of these methods to produce physically realistic cross sections, the fact that all these models rely on a limited database of experimental data mostly in the equilibrium regime casts doubts about their ability to cope with highly-non-equilibrium conditions successfully.

A set of molecular-level chemistry model-processes for use in DSMC has been proposed by Bird.^{1,10} These processes are based solely on fundamental properties of the colliding molecules, including the available collision energy, molecular dissociation energies, and quantized vibrational energy levels. These event-driven processes link chemical-reaction cross sections to the energy-exchange process and the probability of transition between vibrational energy states. Application of the Generalized Larsen-Borgnakke (GLB) procedures for collisions between molecules that could lead to endothermic dissociation reactions is conceptually straightforward, whereas for exchange reactions it is more speculative. These procedures and the principle of microscopic reversibility are then used to calculate simple event-driven models for recombination and for the reverse (exothermic) reactions that do not require any macroscopic data with a procedure that seeks to balance the flux into and out of each state.

1. Dissociation and Recombination Reactions

The introduction of quantum vibrational states in DSMC procedures¹ proved to be a significant improvement since it allowed a more realistic representation of the energy in the lower widely-spaced vibrational energy levels. The next step was to link the vibrational excitation to the dissociation procedures. Bird¹ suggests that dissociation reactions are part of the process of energy exchange between the colliding molecules. In the light of this, the exchange of vibrational energy is incomplete and inconsistent without linking it to molecular dissociation. This concept is captured in an energy threshold model proposed by Bird.¹ According to this model, if during the energy-exchange process of a diatomic molecule the energy content of the vibrational mode exceeded the energy threshold of the dissociation or exchange reaction, the reaction would occur.

Lord¹⁵ in his critique of Bird's¹ model points out that there is a "continuum", i.e., an infinite number of states above the dissociation limit. Therefore, Lord argues, if a dissociation reaction is energetically possible, it occurs.

Thus, assuming a particular collision between two molecule-simulators, where at least one of them is a molecule, the serial application of the GLB energy exchange model would make energy:

$$E_c = E_{trans,pair} + E_{vib,mol} \quad (1)$$

available to the vibrational mode of the molecule in question. In Equation (1), $E_{trans,pair}$ is the translational energy of the pair and $E_{vib,mol}$ is the vibrational energy of the molecule in question. Assuming a harmonic oscillator model for the vibrational mode, the maximum vibrational level that could be obtained i_{max} is $i_{max} = \text{int}[E_c/(k\Theta_v)]$. If this level is higher than the dissociation level $i_d = \Theta_d/\Theta_v$, where Θ_d is the characteristic dissociation temperature, i.e., if, $i_{max} > i_d$, a dissociation reaction occurs.

Assuming a gas in thermodynamic equilibrium at temperature T and a molecule from this gas at a particular vibrational level i , the probability of the translational energy exceeding the difference between the level i and the dissociation level i_d is given by:

$$P = \frac{\Gamma[(5/2 - \omega), (\Theta_d - (i-1)\Theta_v)/T]}{\Gamma(5/2 - \omega)} \equiv Q[5/2 - \omega, (\Theta_d - (i-1)\Theta_v)/T], \quad (2)$$

where Γ is the incomplete gamma function. Summing these probabilities for all vibrational levels up to the dissociation level i_d , multiplying by the equilibrium collision frequency, and dividing by the number densities of the species, the dissociation rate coefficient is obtained:

$$k(T) = \frac{2\sigma_{ref}}{\varepsilon\sqrt{\pi}} \left(\frac{T}{T_{ref}} \right)^{1-\omega} \left(\frac{2k_B T_{ref}}{m_r} \right)^{1/2} \sum_{i=0}^{i_d} \left\{ Q \left[\left(\frac{5}{2} - \omega \right), \left(\frac{\Theta_d - (i-1)\Theta_v}{T} \right) \right] \right\} \frac{\exp(-i\Theta_v/T)}{z_{vib}(T)}, \quad (3)$$

where $z_{vib} = \{1 - \exp(-\Theta_v/T)\}^{-1}$ is the vibrational partition function in the harmonic oscillator model, σ , ω , and m_r are the collision cross section, viscosity temperature exponent, and reduced mass of the pair, respectively, and ε is a symmetry parameter that is set to 1 for like molecules and to 2 for unlike molecules.

The model does not explicitly account for the effect of rotational energy participating in the dissociation process. It is known that high rotational energies can stimulate dissociation both by reducing the dissociation energy threshold due to the centrifugal effect and by affecting the dynamics of collisions between rapidly rotating molecules. However, because rotational and translational energies quickly equilibrate, the rotational energy may effectively participate in the process through the translational energy according to Equation (1).

For the fraction of collisions that can be regarded as three-body collisions, the condition for recombination is as follows. Recombination occurs in a collision between the appropriate atoms if the potentially recombined molecule after a trial GLB redistribution of the relative translational energy of the atom-atom pair is found to be at the ground vibrational state. The addition of the dissociation energy to this molecule would then bring it to the state appropriate for dissociation. A three-body collision is considered to occur if a third molecule-simulator is found within the collision volume of a colliding pair. There is no unambiguous definition of the collision volume. For the purposes of this study and treating the radius of a molecule as its sphere of influence, the collision volume of a colliding molecule is assumed to be that of a sphere having as radius the effective radius of the colliding atoms. The ratio of the collision volume to the cell volume gives the probability that a molecule-simulator is found inside this volume, i.e., within the sphere of influence of the colliding atoms. A third molecule-simulator is not actually selected from the population of the cell to take part in this three-body collision. Instead, the recombination probability is based on the properties of the two initial atoms. Thus, the third colliding partner does not have any effect on the available energy of the collision.

2. Endothermic and Exothermic Exchange Reactions

Similarly, endothermic exchange reactions take place when the vibrational level of the colliding molecule after a trial GLB redistribution of energy E_c , as given by Equation (1), is one level above the level corresponding to the activation energy E_a :

$$i = i_a = \text{int}[E_a / k_B \Theta_v] + 1, \quad (4)$$

where i_a is the first vibrational level above the energy threshold of the reaction.

For example, for an endothermic exchange reaction such as $N_2 + O \rightarrow NO + N$ with activation energy E_a , a reaction takes place if, in an N_2 and O collision, the vibrational level of N_2 after a redistribution of energy is above the reaction activation energy level. The activation energy of the exchange reaction is much smaller than that of the dissociation reaction. The macroscopic rate at which this process occurs can be readily derived:

$$k(T) = \frac{2\sigma_{\text{ref}}}{\varepsilon\sqrt{\pi}} \left(\frac{T}{T_{\text{ref}}} \right)^{1-\omega} \left(\frac{2k_B T_{\text{ref}}}{m_r} \right)^{1/2} \exp\left(-\frac{i_a \Theta_v}{T}\right) / z_{\text{vib}}(T). \quad (5)$$

Physically realistic molecule-level processes such as these can be implemented in standard DSMC codes. This approach makes no use of any macroscopic reaction-rate data and bases the calculation of the dissociation, recombination, and exchange reaction cross sections on kinetic theory and known microscopic data. The fact that the model is introduced in an inherently non-equilibrium method means that arbitrarily chosen non-equilibrium conditions mimicking those encountered by hypersonic vehicles can be simulated and the reactions rates calculated for those conditions.

The law of mass action could be used to determine the cross section of the reverse exothermic reaction, but an event-driven approach based on the principle of microscopic reversibility has overwhelming advantages. Bird¹⁰ suggests that an exothermic exchange reaction takes place when the newly formed molecule after a GLB trial redistribution of the total collision energy including the reaction energy E_a is formed at the vibrational state corresponding to the activation energy as in Equation (4).

III. Application to Particular Reactions

In this Section, the validity of the event-driven approach is investigated by selecting a reduced-chemistry system representative of hypersonic reacting flows for which suggested reaction rates exist. The reliability and accuracy of these rates can be argued. In fact, very few of these reactions have error estimations, and all of them are highly questionable at temperatures above 10,000 K. Nonetheless, this data set represents state-of-the-art knowledge for the rates of these reactions.

In Section III.A, DSMC reaction rates calculated under conditions of thermodynamic equilibrium are compared against available measurements to confirm that the proposed approach can produce reliable results. Comparisons to actual cross sections would be ideally needed to evaluate the new model. However, rate information is more commonly used and therefore more easily accessible for all reactions of interest. Subsequently, in Section III.B, the new method is used to produce non-equilibrium reaction-rate information model appropriate for comparison to non-equilibrium chemical reaction rates, semi-empirically or semi-theoretically derived, and to experimentally measured rates. For the second set of comparisons, the vibrational energy is distributed according to the Boltzmann (equilibrium) distribution but at a different temperature than the translational-rotational mode.

The DSMC chemistry model procedures are implemented in a zero-dimensional DSMC code. Since the collision phase in DSMC is a procedure that involves only molecules within a cell, unlike the move phase, only a single cell need be considered. When two or more simulators are picked for collision, the probability of a chemical reaction occurring is calculated. Through a comparison with a random number, the decision is made as to whether or not a chemical reaction should occur. If it does, the number of reactions is advanced by one, but, unlike ordinary practice, the identities of the molecule simulators are not changed. All the results presented herein were obtained using 10^6 molecule-simulators, with their properties sampled from the equilibrium distribution at the appropriate temperature. To enhance the statistical sample, and only for the equilibrium temperature cases, molecules after a collision are allowed to redistribute their energy between the available modes. For the non-equilibrium case, energy exchange was allowed only between the three degrees of freedom of the translational mode, keeping the total translational energy of the molecule constant while redistributing it among its three components.

It should be noted that, whatever energy redistribution between the colliding molecules is employed, since the zero-dimensional code does not involve interactions with solid boundaries, the system is adiabatic, and the total energy of the cell remains constant and equal to the initial energy of the cell throughout the calculation. This may have a visible effect for high-temperature simulations of low-energy threshold reactions, where a relatively small

statistical variation of the total energy may lead to a small but measurable deviation of the equilibrium collision and reaction rate from the equilibrium one.

A. Equilibrium Reaction Rates for Atmospheric Reactions

The ability to reproduce known equilibrium reaction rates is a necessary condition for any chemistry model. The compilation of reaction rates by Park² is currently considered the most reliable set of reaction rates available. Most of the experimental data, on which the reaction-rate set is based, were obtained for low temperatures (2,000-7,000 K). Park,² through careful study and comparison with numerical simulations, suggests that the experimentally obtained reaction rates can be extrapolated up to 30,000 K, if necessary. Due to the variety of measurement techniques and methodologies used in obtaining these rates, the accuracy of the measurements cannot be easily determined. According to Park, most of these rates should be considered reliable within a factor of 3-10. In some cases, significantly different fittings of the Arrhenius-rate functional form to the same data have been presented.

1. Dissociation Reactions

The main dissociation reactions in hypersonic applications are the dissociation of O_2 and N_2 and to a lesser extent, due to its small concentration, NO . Having a lower dissociation threshold, O_2 is the first species to react, followed by N_2 . Due to the low dissociation threshold of O_2 , its dissociation reaction has been studied more thoroughly than any other reaction. Adequate measurements also exist for the dissociation of nitrogen. The dissociation of nitric oxide is not as well known. Although nitric oxide is a molecule that can be detected through radiation, its dissociation rate is not well known due to competing reactions that take place.

Figure 1-Figure 3 present the dissociation reactions of O_2 , N_2 , and NO . Figure 4-Figure 6 present the dissociation reaction rates of the same species due to collisions with atomic oxygen and atomic nitrogen. The red lines and circles represent the results obtained using the new model with its analytical expression, Equation (3), and its DSMC implementation, respectively. The blue lines represent the reaction rates suggested by Park using his two-temperature model. The green lines represent the experimental measurements Park used to derive his set of reaction rates using a multi-temperature model.

It is indicative of the uncertainty related to these rates that the single-temperature interpretations of the original data are different from Park's two-temperature interpretation, which is almost invariably used for hypersonic applications. In Figure 1-Figure 6, the rates are extrapolated to either 30,000 K or 20,000 K. Park suggests that, in a real non-equilibrium flow field, the vibrational temperature is always lower than the translational temperature. Thus, even in cases where the translational temperature reaches 50,000 K, the vibrational temperature hardly reaches 10,000 K (at that temperature, O_2 is completely dissociated), bringing the geometric average temperature to about 20,000 K. Extrapolating these rates to 30,000 K, which is significantly above the range where measurements exist, must be considered questionable.

The accuracy associated with these measured rates is not always reported and in some cases not even known. The problem becomes even more severe in the temperature range ($T \geq 10,000$ K) where these rates are extrapolated. Park reports that some of the measured reaction rates, for the same reaction, differ by more than one order of magnitude. Based on this observation and for the purpose of facilitating meaningful comparisons with calculated rates, measured and extrapolated reaction rates are herein assumed to be accurate to one order of magnitude. Thus, an uncertainty of one order of magnitude has been assigned to measured and extrapolated rates in Figure 1-Figure 6. This uncertainty is designated by error bars.

Based on this presumed accuracy of all measurements, DSMC results (points or solid lines) are generally in good agreement with Park's rates. In fact, the DSMC results may actually be in better agreement with the original data than with Park's interpretation of them. The differences between Park's interpretation of the data and the original data themselves are in almost all cases within the range of uncertainty associated with the measured data. It is not clear therefore, whether the observed better agreement of the DSMC results with the original data can be considered systematic or fortuitous.

Based on the results of Figure 1-Figure 6, no unambiguous conclusion can be drawn about the effect of the absence of the rotational energy from the formulation of the model. While atom-molecule dissociation reactions appear to be under-predicting equilibrium reaction rates, exactly the opposite is observed for molecule-molecule reactions.

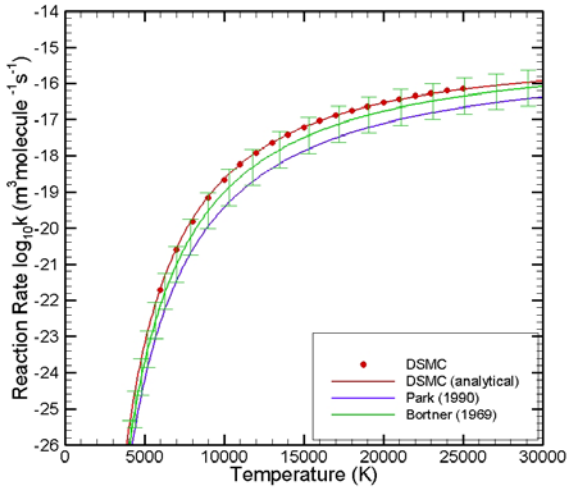


Figure 1. Nitrogen dissociation:
 $N_2 + N_2 \rightarrow N + N + N_2$.

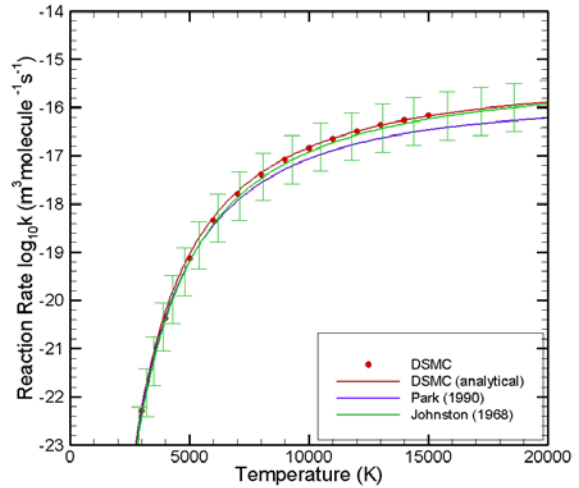


Figure 2. Oxygen dissociation:
 $O_2 + O_2 \rightarrow O + O + O_2$.

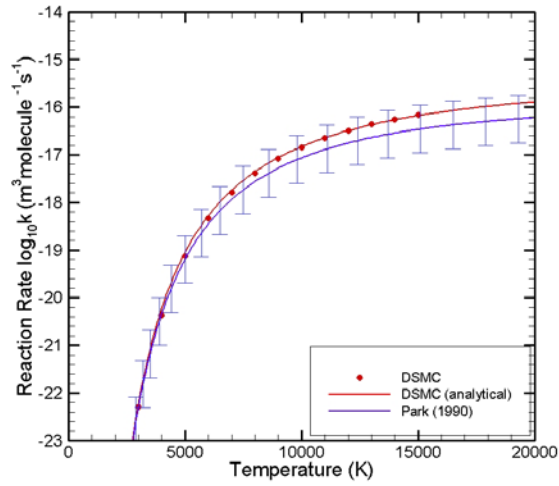


Figure 3. Nitric oxide dissociation:
 $NO + NO \rightarrow N + O + NO$.

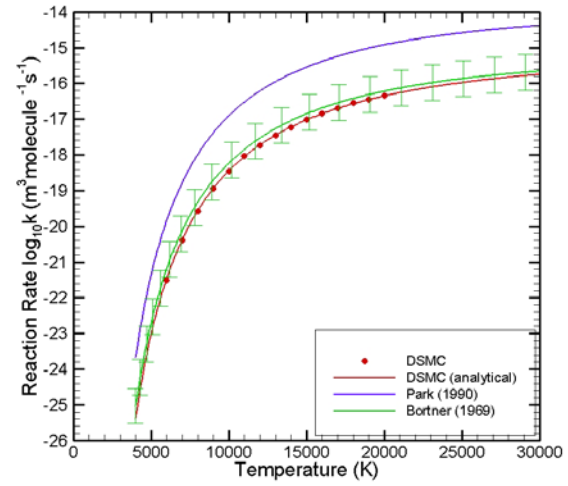


Figure 4. Nitrogen dissociation by atomic nitrogen:
 $N_2 + N \rightarrow N + N + N$.

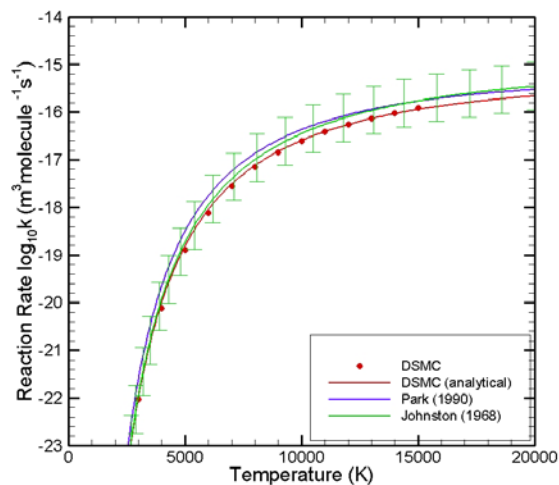


Figure 5. Oxygen dissociation by atomic oxygen:
 $O_2 + O \rightarrow O + O + O$.

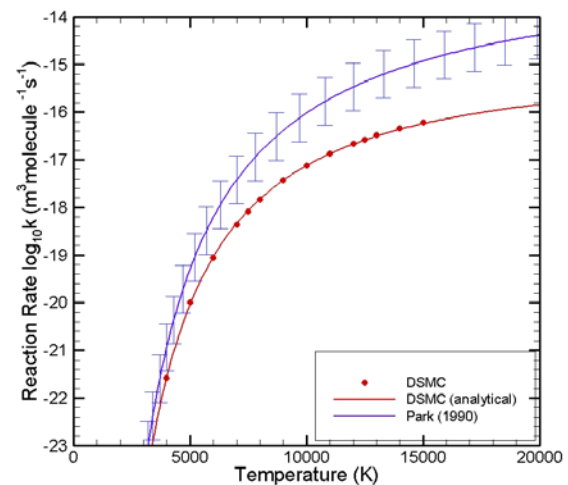


Figure 6. Nitric-oxide dissociation by atomic nitrogen:
 $NO + N \rightarrow 2N + O$.

2. Recombination Reactions

Recombination reactions are the reverse of dissociation reactions and are usually ignored in typical rarefied hypersonic applications due to their low probability of occurrence. Figure 7 and Figure 8 present the recombination reaction rates of atomic oxygen and atomic nitrogen as functions of temperature at equilibrium conditions. For this type of reaction, no analytical representation of the DSMC model is available. The DSMC rates are compared with the reaction rates given by Gupta et al.⁶ They provide a better fit to the equilibrium reaction constant K_{eq} , calculated using the partition-function approach of Park.² The reaction rates Gupta et al. provide are based on their fit of the equilibrium reaction constant and the data of Bortner.⁷ As in the previous section, in Figure 7 and Figure 8 an uncertainty of one order of magnitude has been assigned to the measured rates to indicate the relative error of the proposed procedures.

The oxygen recombination rate is in good agreement with the rate proposed by Gupta et al.⁶ A larger difference, but still less than one order of magnitude, which is the presumed accuracy of the measured rates, is observed for the case of nitrogen recombination.

The model for recombination reactions has the disadvantage of using the ambiguous collision volume (Section II.A.1) to calculate the three-body collision rate. Bird¹⁰ assumed the radius of the collision volume to be about 2-3 times the radius of the molecule. As stated in Section II.A.1, herein, the radius of a DSMC molecule-simulator is assumed to be its sphere of influence, which is thus employed as the radius of the collision volume. Assuming a larger volume would raise the collision probability and therefore the reaction rates, bringing the DSMC nitrogen recombination reaction rate into better agreement with the rates calculated using the equilibrium reaction constant and the measured reverse reaction rates for all temperatures. Similarly, in the vicinity of 15,000 K, using the larger collision volume would bring the oxygen recombination rate into better agreement with the rates calculated using the equilibrium reaction constant and the measured reverse reaction rates.

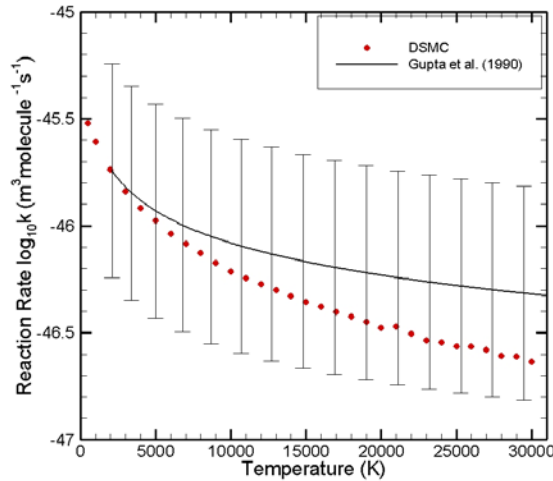


Figure 7. Atomic oxygen recombination:
 $O + O + O \rightarrow O_2 + O$.

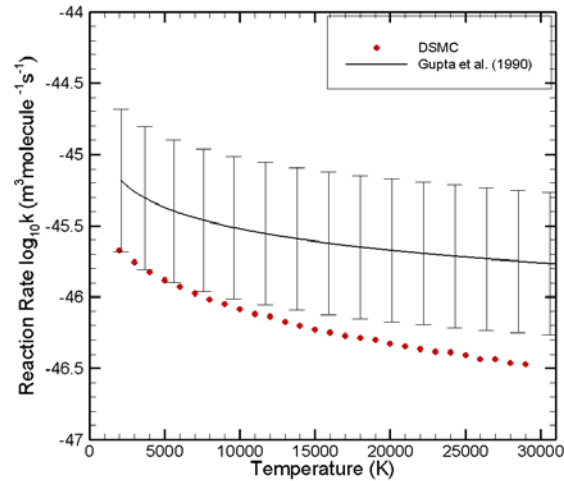


Figure 8. Atomic nitrogen recombination:
 $N + N + N \rightarrow N_2 + N$.

3. Endothermic Exchange Reactions

Figure 9 and Figure 10 present the reaction rates of the endothermic exchange reactions



These reactions are critical for hypersonic applications since, because of their low energy threshold, they are mainly responsible for the formation and depletion of nitric oxide, which is a major radiating species in hypersonic flow fields. For both reactions, DSMC predictions are found to be in very good agreement with the measured rates.

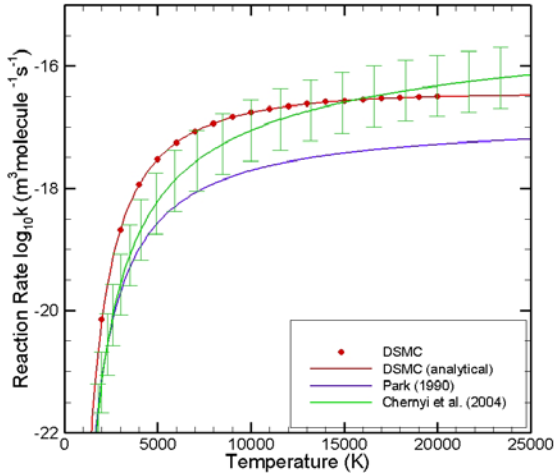


Figure 9. Nitric-oxide/oxygen endothermic exchange reaction: $NO + O \rightarrow O_2 + N$.

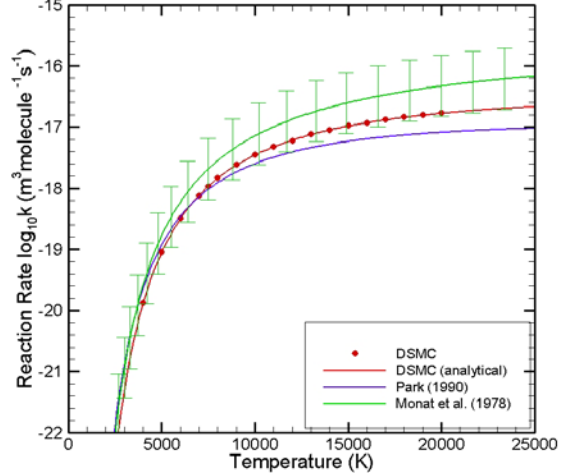


Figure 10. Nitrogen/atomic-oxygen endothermic exchange reaction: $N_2 + O \rightarrow NO + N$.

The differences between the Park² rates and the measured rates become significant for these reactions, especially at high temperatures. These reaction rates have been measured only at relatively low temperatures, below 4,000 K. Park, based on a variety of data and numerical simulations, proposes a reaction rate with an arbitrary value for the temperature exponent of -1 and suggests that this should be reliable up to 30,000 K. Park also suggests that, for hypersonic flows where the temperature reaches a value of 30,000 K, the vibrational temperature should be limited to around 7,000 K, resulting in an average temperature of 15,000 K. The rate for the reaction in Equation (6) is also compared to the rate measured by Monat et al.¹⁶ The measured reaction rate has an uncertainty of about 35% in the temperature range 2,384–3,850 K and thus is considered to be one of the best known reaction rates. Other measurements for this reaction are all within a factor of 3. Since the error of these rates in the extrapolated region of the temperature domain is not known and in harmony with Park's suggestions, all measured and extrapolated rates are assumed to be accurate to within one order of magnitude. This is reflected by the one-order-of-magnitude-wide error bars assigned to the measured rates in Figure 9 and Figure 10.

The DSMC rate at 3,800 K was found to differ by 51% from the measured value. Although this difference is marginally outside the bounds of measurement error, it is well within the one-order-of-magnitude error projected for these reactions.

4. Exothermic Exchange Reactions

Exothermic exchange reactions are the reverse of the reactions studied in the previous section, namely Equations (6) and (7). No direct measurements for these reverse reactions exist, the reaction rates being estimated from the equilibrium gas constant and the forward reaction rate. Both Park's and Gupta's equilibrium reaction constants are compared the DSMC results in Figure 11 and Figure 12. In both figures, the red symbols present the DSMC reaction rates.

Figure 11 presents the reaction rates for $O_2 + N \rightarrow NO + O$. Gupta et al.⁶ suggest that the reaction rate is constant: $k = 2.4909 \times 10^{-17} \text{ m}^3 \text{molecule}^{-1} \text{s}^{-1}$ ($\log_{10}(k) = -16.60$). The results in Figure 11 are obtained using Park's equilibrium reaction rate constant and Park's and Monat's suggested forward reaction rates.

Figure 12 presents the reaction rates for $NO + N \rightarrow N_2 + O$. Here, the rates suggested by Park and Gupta et al. are compared to the DSMC rates. The different trend of the Gupta et al. rate in Figure 12 is due to a small energy threshold that appears in the reaction rate. No explanation is given for the appearance of this term in the reverse reaction rate. However, in both cases, the DSMC predictions are in reasonable agreement (within one order of magnitude difference) with the theoretical/experimental predictions.

A prominent difference between the DSMC and measured rates is that the DSMC rate increases more gradually with temperature at low temperatures, especially for the reaction $NO + N \rightarrow N_2 + O$ presented in Figure 12. Using the equilibrium reaction constant, a more rapid increase is observed. In fact, according to the equilibrium reaction constants, the rate peaks around 1,000 K and decreases from that point on. The DSMC model produces a more gradual increase up to 5,000–10,000 K, after which the rate appears to plateau. Assuming that these reverse reaction

rates are accurate within one order of magnitude, the DSMC model appears to be in fairly good quantitative agreement with Gupta's rates. For the reverse reactions, Gupta's rates should be considered more accurate than Park's rates since they represent a more rigorous implementation of Park's model (Gupta et al.⁶).

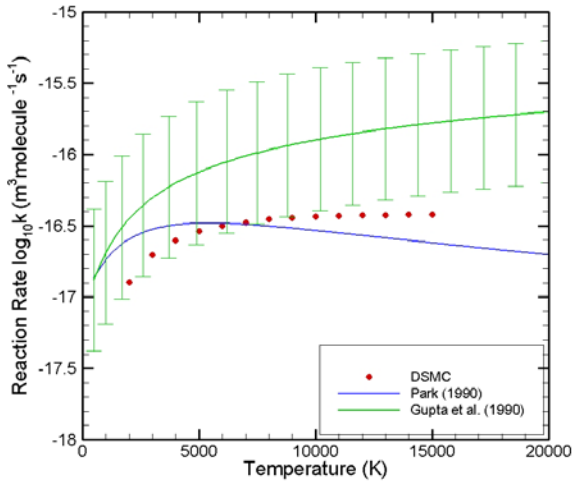


Figure 11. Oxygen/atomic-nitrogen exothermic exchange reaction: $O_2 + N \rightarrow NO + O$.

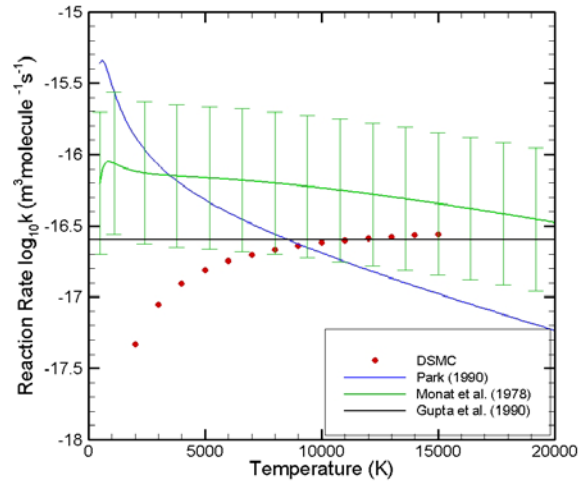


Figure 12. Nitric-oxide/atomic-nitrogen exothermic exchange reaction: $NO + N \rightarrow N_2 + O$.

B. Non-Equilibrium Reaction Rates for Atmospheric Reactions

All cases examined so far involved gases in thermodynamic equilibrium. Although the ability of a chemistry model to reproduce equilibrium chemical reaction rates is a necessary condition, it is not sufficient to demonstrate that the method is capable to reproduce the correct reaction rates when the gas is not in thermodynamic equilibrium. Measured internal-energy-dependent cross sections of reactions between atmospheric species are extremely rare. Some systematic measurements and calculations exist for molecular hydrogen, where the cross section was found (Wadsworth and Wyson¹²) to be significantly affected by the distribution of energy among the reactant molecules. However, due to the relatively more important role of quantum effects in its chemistry, the behavior of hydrogen is expected to deviate from the behavior of heavier, and therefore more classical, atmospheric molecules.

1. Comparison of DSMC and Park's Model

Using the DSMC chemistry model-procedures, arbitrary non-equilibrium conditions can be simulated, and the effective reaction rate under conditions of non-equilibrium can be calculated. The calculation of non-equilibrium reaction rates with the DSMC code entails no differences in modeling since only collision-based molecular-level information is used.

For the study of non-equilibrium reaction rates, the test case selected is similar to the one used for equilibrium calculations, with the only difference being that the vibrational temperature of the gas is set independently from the temperature of the other modes. Thus, the gas is characterized by two temperatures, T_{tr} describing the translational and rotational modes, and T_{vib} , describing the vibrational mode. The energy states are distributed according to the Boltzmann distribution for the internal modes and the Maxwell distribution for the translational modes. These conditions simulate, to some degree, the state of the gas in a Navier-Stokes non-equilibrium calculation.

Figure 13 and Figure 14 present non-equilibrium reaction rates for oxygen and nitrogen dissociation at four translational-rotational temperatures (3,000 K, 5,000 K, 10,000 K, and 15,000 K). Blue, green, red, and black in Figures 15 and 16 designate calculations at translational-rotational temperatures of 15,000 K, 10,000 K, 5,000 K, and 3,000 K, respectively. For each of these temperatures, the vibrational energy was distributed according to the harmonic oscillator model at a temperature that varied from 500 K to 15,000 K for oxygen and 1,000 K to 17,500 K for nitrogen. In both figures, the solid symbols represent the DSMC results. The solid lines in the figures represent Park's two-temperature reaction-rate model for non-equilibrium conditions, i.e., where the temperature in the Arrhenius rate suggested by Park is given by

$$T = T_{tr}^q T_{vib}^{1-q}, \quad (8)$$

with $q = 0.5$. The dashed lines present the measured equilibrium reaction rate at the average temperature (see Section III.B.2). The solid and dashed lines do not intersect at the point of thermodynamic equilibrium, i.e., where $T_{tr} = T_{vib}$. This is a result of Park's suggested rates not fully conforming to the measured rates. Park's method yields good results at high temperatures for both species. However, a discrepancy of several orders of magnitude appears for temperatures below 5,000 K.

The temperature regime of these figures is probably the most critical in modeling hypersonic flow fields since it mimics the conditions behind a shock layer (high translational temperature, low vibrational temperature). Assuming a typical high-altitude hypersonic flow field where the vibrational temperature is initially negligible, the flow will sweep the vibrational temperature regime from left to right in the figure. Thus, a poor estimate of the reaction rates in this initial temperature regime will yield lower dissociation of oxygen. The dissociation of oxygen is usually the first reaction that takes place in the flow field and is followed by the exchange reaction $N_2 + O \rightarrow NO + O$. Results based on underestimated dissociation reaction rates predicted by Navier-Stokes codes using Park's model yielded significantly lower (200 times) NO concentrations in the domain compared to flight measurements.¹⁷

Fitting the DSMC results by Park's Arrhenius-rate type of equation and using the temperature in Equation (8) with q as an adjustable parameter yields q values of 0.78 and 0.7 for oxygen and nitrogen, respectively. The resulting rates using these fittings appear in Figure 15 and Figure 16 for oxygen and nitrogen respectively. The color scheme in these figures follows the pattern of Figure 13 and Figure 14. The non-equilibrium reaction rates using Park's model with the fitted values of q are in better agreement with the DSMC values, especially for temperatures less than 5,000 K. This indicates that a weaker dependence of the average temperature on the vibrational temperature may be more accurate and that multi-temperature effects on dissociation reaction rates may be smaller than initially anticipated, as previously suggested by Sharma et al..

Figure 17 and Figure 18 present the rates for the $N_2 + O \rightarrow NO + N$ and $NO + O \rightarrow O_2 + N$ exchange reaction, respectively. Again, the color pattern of Figure 13 and Figure 14 is followed. Park's model appears to be in agreement with the DSMC rates for near-equilibrium conditions although the discrepancy in the lower vibrational-temperature regime observed for dissociation reactions is observed here as well. In the absence of non-equilibrium validation data, a comparison between two numerical models cannot produce unambiguous conclusions about the validity of either method. Further evidence, introduced by comparison to other theoretical models in Sections III.B.3, will allow for further conclusions to be drawn.

2. Comparison of DSMC and Arrhenius Rates at the Average Temperature

For a gas not in a uniform steady state, the temperature T at any point is defined⁹ as that for which the same gas, when in uniform steady state at the same density, would have the same mean thermal energy per molecule. Thus, the Chapman-Enskog (CE) definition of temperature for a gas that is not in thermal equilibrium is:

$$T = \frac{3 T_{tr} + \zeta_{rot} T_{rot} + \zeta_{vib} T_{vib}}{3 + \zeta_{rot} + \zeta_{vib}}. \quad (9)$$

Equation (9) is an expression of the temperature as the average energy among all available internal energy modes. With this interpretation of temperature in terms of the average energy, the Arrhenius rates can provide an estimate of the non-equilibrium reaction rate in the absence of any other information. This interpretation of the Arrhenius reaction rate can also be treated as a limiting case since no preference is given to any particular mode in promoting a reaction rate.

In Figure 13-Figure 24, the dashed lines present the measured equilibrium reaction rate at the average temperature. For example, the dashed lines in Figure 13 and Figure 14 are the Arrhenius rates of Johnston¹⁹ and Bortner⁷ for oxygen and nitrogen dissociation, respectively. The DSMC data have not been fitted to the measured equilibrium reaction rates, so the differences between the measured and DSMC rates are due to the differences in their predictions for equilibrium conditions.

It is observed that, for high-temperature cases, this simple interpretation of the temperature in the Arrhenius rates as the average energy sufficiently captures non-equilibrium effects, resulting in reaction rates that match the DSMC rates. The agreement breaks down at lower vibrational temperatures, where the agreement is good only in the near-equilibrium regime.

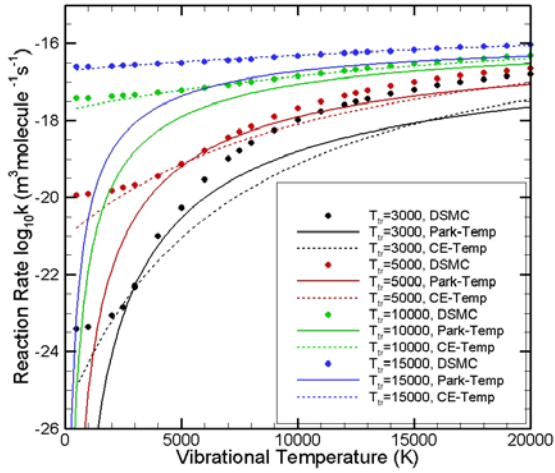


Figure 13. Oxygen dissociation. DSMC and Park's model.

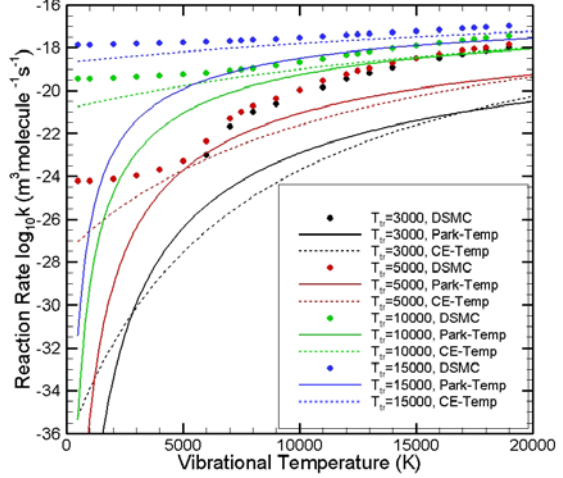


Figure 14. Nitrogen dissociation. DSMC and Park's model.

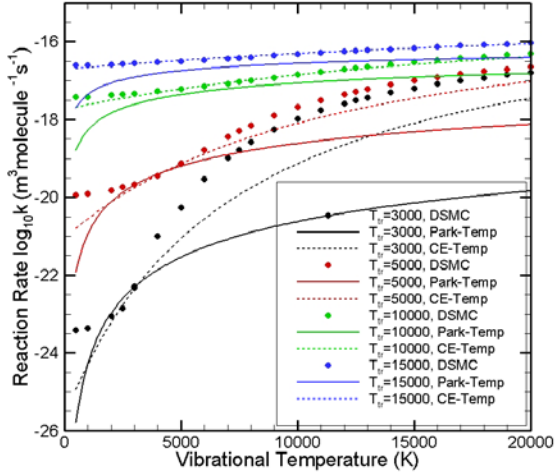


Figure 15. Oxygen dissociation. DSMC and Park's model fit using $q = 0.78$.

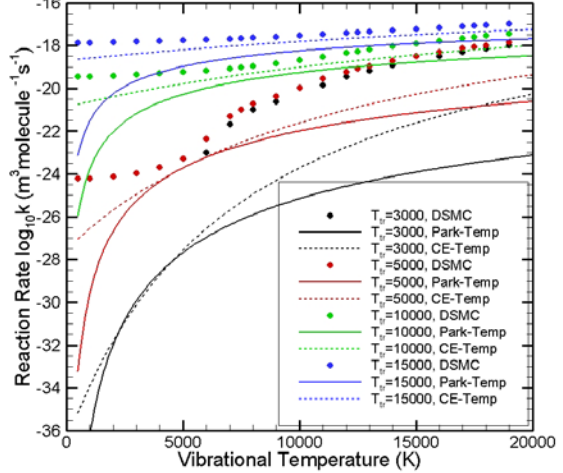


Figure 16. Nitrogen dissociation. DSMC and Park's model fit using $q = 0.7$.

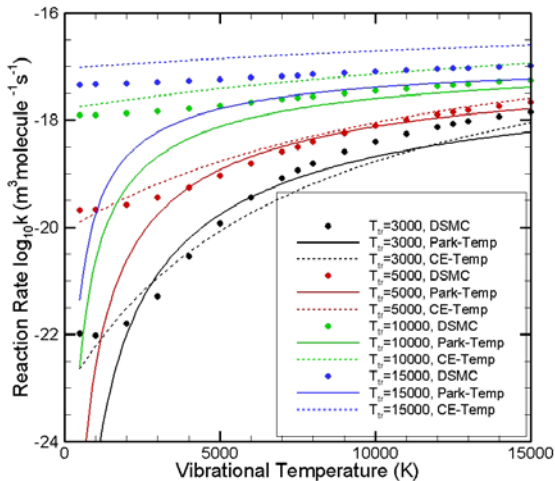


Figure 17. $N_2 + O \rightarrow NO + N$ exchange reaction. DSMC and Park's model.

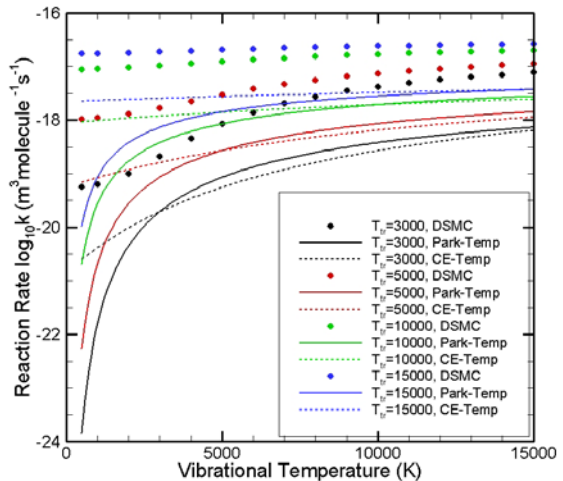


Figure 18. $NO + O \rightarrow O_2 + N$ exchange reaction. DSMC and Park's model.

The agreement between the DSMC non-equilibrium reaction rates and the Arrhenius rates using the CE definition of the average temperature is not a tautology because the DSMC rates are unaware of the macroscopic reaction rate. The agreement also cannot be considered a validation of the DSMC procedures. When replacing the equilibrium temperature in the Arrhenius rate with the average temperature, it is implicitly assumed that the reaction rate is driven by the total available energy. This assumption is a good approximation of Bird's¹⁰ scheme at higher temperatures, where all energy modes have enough energy to overcome the reaction threshold. Therefore, this agreement could be considered a verification of the DSMC procedures.

The suggestion that reaction rates are mainly influenced by the total energy available in reactants ostensibly conflicts with the notion that chemical reactions, and in particular dissociation reactions, are strongly influenced by the energy content of the vibrational energy mode since strong evidence exists that individual reactions are significantly influenced by the energy configuration of the reactants. However, it appears that, for highly energetic collisions, the energy exchange that takes place during a collision may somewhat mask this effect. In fact, theory¹⁸ supported by experiments suggests that, while for low collision energies the selective energy requirements can significantly influence the reaction rate, at higher collision energies the energy requirements become less restrictive. Thus, for high temperatures, the availability, or not, of sufficient total collision energy to overcome the energy barrier for the reaction to proceed appears to be strongly influencing the reaction probability.

3. Comparison of DSMC and Non-Equilibrium Reaction Models

Significant effort has been expended in attempts to express the dependence of the rate constant on the degree of vibrational excitation through the non-equilibrium factor:

$$k(T_{tr}, T_{vib}) = k(T)Z(T_{tr}, T_{vib}), \quad (10)$$

where the subscripts *tr* and *vib* denote the translational and vibrational energy modes, respectively. Many theoretical and semi-empirical theories provide estimates for the non-equilibrium deviational parameter $Z(T_{tr}, T_{vib})$. Some of these models make use of empirical or adjustable parameters that are estimated based on experimental data or quantum mechanical computations, and some require only microscopic information. In general, these models can be divided into two categories:

- i) Intuitive models, such a Park's model examined in the previous section, aim at providing an estimate of non-equilibrium effects based on experimental observations.
- ii) Theoretical models describe the physical processes using simple mechanisms that provide insight into the role of vibrational energy in promoting chemical reactions.

The existing intuitive and theoretical models for dissociation reactions are more advanced than those for exchange reactions. Both classes of models have been extensively reviewed in the literature (Chernyi et al.⁸, Pogosbekian et al²⁰).

One of the most general models based entirely on theoretical considerations is the Adiabatic Dissociation Model (ADM) of Smekhov et al.⁸). The model assumes that the energy states are distributed according to the Boltzmann distribution for the internal modes and the Maxwell distribution for the translational modes. The vibrational modes and the translational modes are each characterized by a single but distinct temperature. The model assumes that dissociation can occur from any vibrational level, including the ground state. However, the energy threshold is a function of the translational energy, compensating in this way for the intra-molecular energy transfer that can take place during a collision. The dissociation cross section is given by the Massey adiabatic parameter as $\sigma = \sigma_T \exp(-\xi)$, where σ_T is the total cross section and ξ is a function of the translational energy (Chernyi et al.⁸ 2004). The vibrational mode is described by the Morse anharmonic oscillator model.

Figure 19 and Figure 20 present the DSMC and ADM results for oxygen and nitrogen dissociation respectively. The ADM results are given by solid lines, where blue, green, red and black designate translational-rotational temperatures of 15,000 K, 10,000 K, 5,000 K, and 3,000 K, respectively. The ADM non-equilibrium rates have been calculated as deviations from the measured equilibrium rates of Johnston¹⁹ for oxygen and Bortner⁷ for nitrogen, which is how results would be obtained if these models were used in a Navier-Stokes code having knowledge of only the measured equilibrium reaction rates. The dashed lines present the measured equilibrium reaction rates, where the equilibrium temperature is replaced with the CE temperature of Equation (9).

It is observed that the ADM model, especially for low temperatures, is in very good agreement with the DSMC calculated rates. The lack of agreement for the higher temperatures can be attributed to the harmonic oscillator model used in the DSMC model to describe the vibrational mode. The agreement for oxygen is better than that for nitrogen because the DSMC results are in better agreement with the measured rates used as the equilibrium rate for the ADM model.

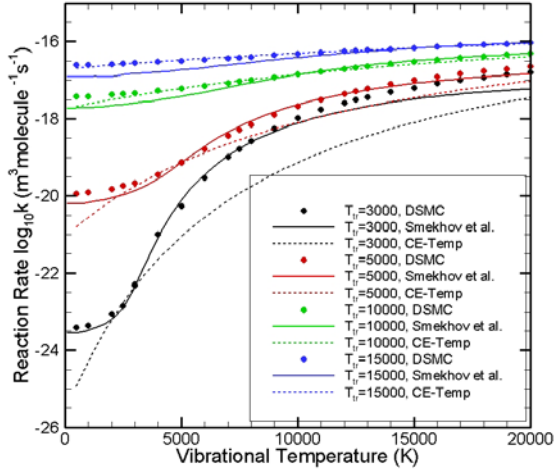


Figure 19. Oxygen dissociation. DSMC and ADM model.

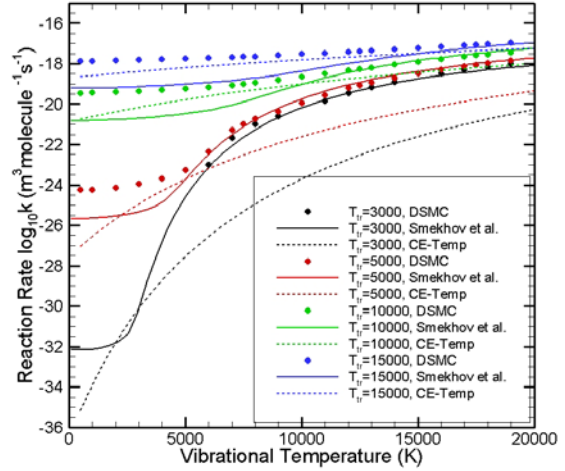


Figure 20. Nitrogen dissociation. DSMC and ADM model.

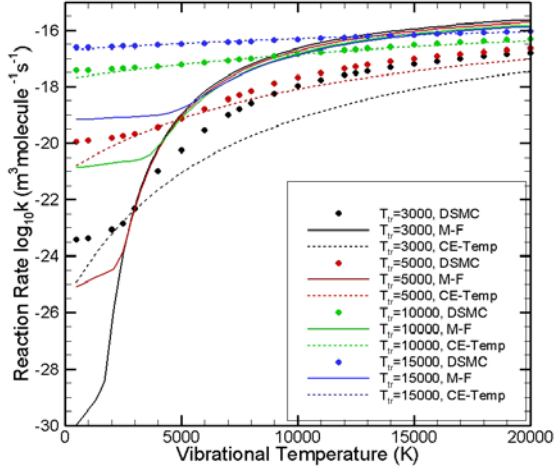


Figure 21. Oxygen dissociation. DSMC and Macheret-Fridman model.

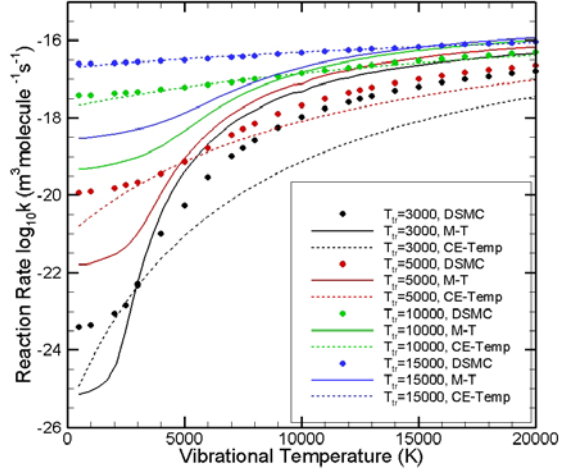


Figure 22. Oxygen dissociation. DSMC and Marrone-Treanor model.

Figure 21 and Figure 22 present similar comparisons between DSMC and the oxygen dissociation models of Macheret and Fridman (M-F) and Marrone and Treanor (M-T) (in Chernyi et al.⁸), respectively. The Macheret-Fridman model uses two distinct dissociation mechanisms, one from the lower vibrational levels and another from the upper vibrational levels. The translational energy plays a critical role for dissociation from the lower vibrational levels. Dissociation occurs only for particular relative configurations of colliding molecules that minimize the energy barrier. The Macheret-Fridman model has been shown to produce deviations from the experimental data in excess of one order of magnitude, a behavior observed here in the low-vibrational-temperature regime. The Marrone-Treanor model uses a truncated harmonic oscillator to describe the vibrational mode and assumes that dissociation can occur from any vibrational state without distorting the Boltzmann distribution of molecules over vibrational levels. The Marrone-Treanor model contains a free parameter that must be estimated by comparison with experimental data or quantum mechanical calculations. According to Capitelli et al.²¹, this adjustable parameter has

to be a function of the translational temperature and the vibrational level for the model to produce results in agreement with quantum mechanical calculations. Even in this case, and in harmony with the results of Figure 22, the Marrone-Treanor model was found to underpredict reaction rates for low vibrational temperatures. Both the Macheret-Fridman and Marrone-Treanor models are limited to vibrational temperatures lower than the translational-rotational temperature. The values for the adjustable parameters employed in both models are the ones suggested by Chernyi et al.⁸

The various theoretical models predict significantly different reaction rates at low vibrational temperatures. Evidently, the discrepancy between the predictions of the ADM, Macheret-Fridman, and Marrone-Treanor models is related to differences in allowing translational energy to promote dissociation reactions from low vibrational states.

Figure 23 and Figure 24 present similar calculations for the exchange reactions of Equations (6) and (7). The DSMC non-equilibrium reaction rates here are compared to the α model (Chernyi et al.⁸). The α - model predictions are given by solid lines with color corresponding to the translational temperature. The α model assumes that vibrational energy plays a limited role in the reaction and only a fraction of it (α) participates in overcoming the energy threshold, whereas the translational energy is fully utilized in overcoming the energy threshold.

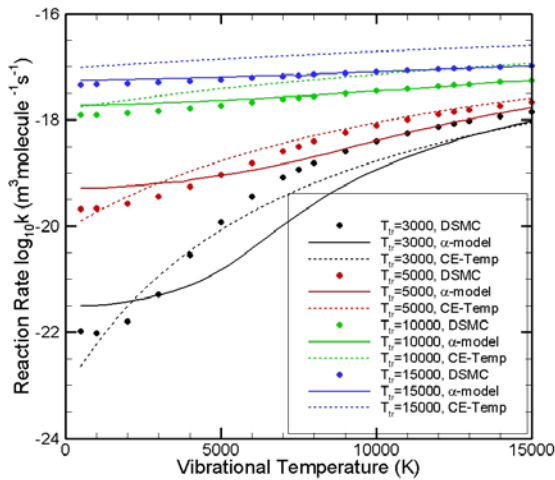


Figure 23. $N_2 + O \rightarrow NO + N$ exchange reaction.
DSMC and DSMC-calibrated α model.

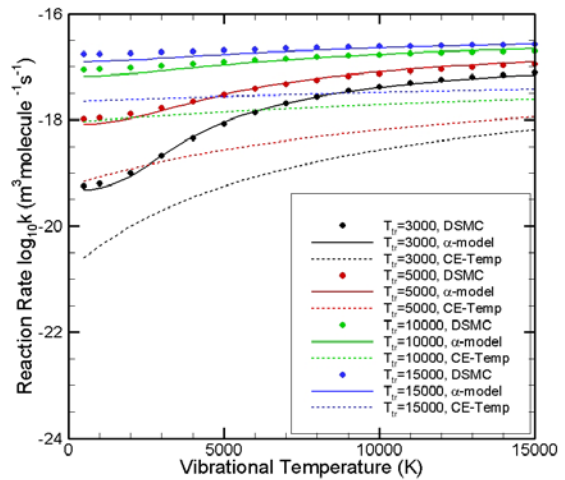


Figure 24. $NO + O \rightarrow O_2 + N$ exchange reaction.
DSMC and DSMC-calibrated α model.

Figure 23 and Figure 24 present the comparisons of the α model to DSMC and average-temperature reaction rate, where the α model has been calibrated to the DSMC equilibrium reaction rate. It is observed that the α model, produces non-equilibrium reaction rates that are in very good agreement with DSMC non-equilibrium rates. As pointed out earlier in this section, this agreement cannot be considered a validation of either of the two models. However, based on the similarity of the two models, useful conclusions can be drawn about these models. The α fraction of the vibrational energy that participates in overcoming the energy threshold in addition to the translational energy could be related to the average vibrational energy that is disposed to the vibrational mode of the potentially formed products of the reaction. Chernyi et al.⁸ give values of $\alpha = 0.51$ and 0.94 for the reactions in Equations (6) and (7). Chernyi et al. also point out that for endothermic reactions α is expected to be in the interval $0.9 \leq \alpha \leq 1.0$. This may be the reason the agreement of this model with DSMC is better for the reaction in Equation (7) (Figure 24), where $\alpha = 0.94$, than for the reaction in Equation (6) (Figure 23), where $\alpha = 0.51$.

The agreement between DSMC and the α model in the low-vibrational-temperature regime is due to the fact that both models allow the translational energy alone to be used to overcome the energy threshold of the reaction, unlike Park's model, which predicts vanishing reaction rates as the vibrational temperature tends to zero. This difference between DSMC and Park's model is particularly important since in hypersonic reentry flow fields the free-stream vibrational temperature is typically negligible. Thus, any shock layer would necessarily go through the small vibrational temperature non-equilibrium regime presented on the left side of Figure 13-Figure 25.

4. Comparison of DSMC and Measured Non-Equilibrium Reaction Rates

Very limited data are available for atmospheric species reaction rates under conditions of non-equilibrium. Sergievskaya et al.²² report a small number of dissociation reaction rates obtained from shock-tube measurements that involve atmospheric species.

Figure 25 presents measurements reported by Sergievskaya et al.²² for oxygen dissociation. The measurements presented with green lines in Figure 25 are upper and lower limits of the reaction rate. The spread of the measurements is somewhat below one order of magnitude. The vibrational temperature in these experiments was kept constant at 4,200 K while the translational and rotational temperatures were kept in equilibrium with each other. The non-equilibrium rates are presented in the form of the deviational parameter Z of Equation (10). Figure 25 also presents the ratio of the non-equilibrium to the equilibrium reaction rate as calculated by DSMC and Park's model using $q = 0.5$, as originally suggested by Park, and $q = 0.78$, as calculated in this work by fitting Park's model to DSMC data. The left side of the plot, where the blue and red lines intersect, is where the gas is in thermal equilibrium. As the translational temperature increases, the degree of non-equilibrium also increases.

As conditions depart from equilibrium, the DSMC predictions are bounded by the experimental results. Park's original model ($q = 0.5$) deviates from the measurements, when non-equilibrium becomes appreciable. However, adopting a factor of $q = 0.78$ for Park's model brings the non-equilibrium predictions in very good agreement with DSMC predictions.

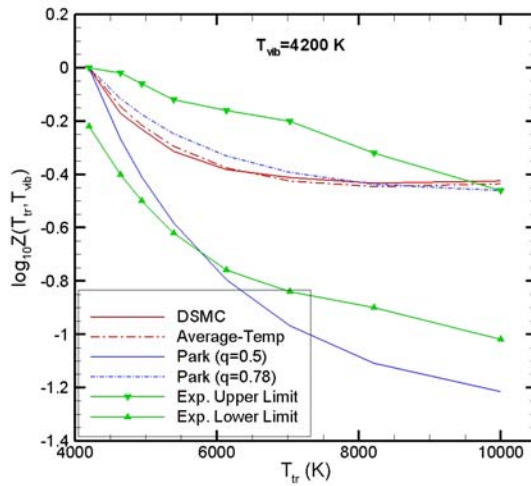


Figure 25. DSMC, Park, and measured non-equilibrium reaction rates.

Although less than one order of magnitude, the spread in the experimental measurements is significant, so an unequivocal assessment of the models cannot be made. However, the measured rates reproduce the trend observed in the previous section for highly non-equilibrium conditions, where the reaction rates were found to reach a plateau as a function of the translational temperature of the gas.

IV. Conclusions

A set of recently proposed procedures to model chemical reactions within the context of the DSMC method has been implemented, verified, and validated. The new model, unlike all other DSMC chemical-reaction models available, does not rely on measured macroscopic reaction rates to calibrate adjustable parameters. Instead, it makes use of the principles of microscopic reversibility and molecular-level energy exchange to predict the probability of a chemical reaction occurring during a collision between two molecules. Based solely on molecular properties and collision energetics, the model cannot account for quantum mechanical effects applying to transitions between energy states.

Through a series of comparisons, it was established that the DSMC models can produce reaction rates in fairly good agreement with the best available measured or extrapolated reaction rates. The experimental uncertainty of the measurements and the idealizing assumptions of the calculations do not allow for an unequivocal assessment of the models in question through these comparisons. However, the discrepancies between the currently most reliable reaction-rate data and the DSMC predictions appear to be always within one order of magnitude. This level of

agreement between the DSMC models and measured and calculated rates is a source of optimism concerning the ability of the method to provide predictions of non-equilibrium reaction rates between these species.

For non-equilibrium conditions, Park's model is the predominant chemical reaction model used in Navier-Stokes calculations. The DSMC model is found to be in very good qualitative and quantitative agreement with theoretical predictions and well within the accuracy of measured non-equilibrium reaction-rate predictions. In fact, the DSMC results indicate that, in agreement with theoretical predictions and experimental observations, the selectivity of a reaction rate on the reactant energy is minimized as the total collision energy increases.

Acknowledgments

This work was performed at Sandia National Laboratories. Sandia is a multiprogram laboratory operated by Sandia Corporation, a Lockheed Martin Company, for the United States Department of Energy's National Nuclear Security Administration under contract DE-AC04-94AL85000.

References

1. G. A. Bird, Molecular Dynamics and the Direct Simulation of Gas Flows, Oxford University Press, Oxford, UK, 1994.
2. C. Park, Nonequilibrium Hypersonic Aerothermodynamics, John Wiley & Sons, New York, NY, 1990.
3. R. A. Dressler, Chemical Dynamics in Extreme Environments, World Scientific, Singapore, 2001.
4. M. A. Gallis and J. K. Harvey, "On the Modeling of Thermochemical Non-Equilibrium in Particle Simulations", *Physics of Fluids*, **10**, (6), pp. 1344-1358, 1998.
5. C. Park, "Review of Chemical-Kinetic Problems of Future NASA Missions, I: Earth Entries", *Journal of Thermophysics and Heat Transfer*, **7**, (3), pp. 385-398, 1993.
6. R. N. Gupta, J. M. Yos, R. A. Thompson, and K.-P., Lee, "A Review of Reaction Rates and Thermodynamics and Transport Properties from an 11-Species Air Model for Chemical and Thermal Nonequilibrium Calculation to 30,000 K", NASA Reference Publication 1232, August 1990.
7. M. H. Bortner, "A Review of Rate Constants of Selected Reactions of Interest in Re-Entry Flow Fields in Atmosphere", NBS TN 484, 1969.
8. G. G. Chernyi, S. A. Losev, S. O. Macheret, and B. V. Potapkin, "Physical and Chemical Processes in Gas Dynamics", Vol. I: Cross Sections and Rate Constants, *Progress in Aeronautics and Astronautics*, **197**, 2004.
9. S. Chapman and T. G. Cowling, The Mathematical Theory of Non-Uniform Gases, Cambridge University Press, Cambridge, UK, 1970.
10. G. A. Bird, "A Comparison of Collision Energy-based and Temperature-based Procedures in DSMC", *Rarefied Gas Dynamics*, 26th Symposium, **1084**, Ed. T. Abe, American Institute of Physics, pp. 245-250, 2009.
11. M. A. Gallis, R. B. Bond, J. R. Torczynski, "A Kinetic-Theory Approach for Computing Chemical-Reaction Rates in Upper-Atmosphere Hypersonic Flows", *Journal of Chemical Physics*, **131**, 124311, 2009.
12. C. Wadsworth and I. J. Wysong, Vibrational favoring effect in DSMC dissociation models, *Physics of Fluids*, **9** (12), pp. 3873-3884, 1997.
13. G. A. Bird, "Simulation of Multi-Dimensional and Chemically Reactive Flows", *Rarefied Gas Dynamics*, Ed. R. Campargue, CEA, Paris, pp. 365-388, 1979.
14. I. J. Wysong, R. A. Dressler, Y. H. Chiu, and I. D. Boyd, "Direct Simulation Monte Carlo Dissociation Model Evaluation: Comparison to Measured Cross Sections", *Journal of Thermophysics and Heat Transfer*, **16**, p. 1, 2002.
15. R. G. Lord, "Modeling Vibrational Energy Exchange of Diatomic Molecules using the Morse Interatomic Potential", *Physics of Fluids*, **10**, (3), pp. 742-746, 1998.
16. J. P. Monat, R. K. Hanson, and C. H. Kruger, "Shock Tube Determination of the Rate Coefficient for the Reaction $N_2 + O \rightarrow NO + N$ ", Proceedings of the 17th Symposium (International) on Combustion, pp. 543-552, 1978.
17. D. Bose and G. V. Candler, Thermal Rate Constants of the $N_2 + O \rightarrow NO + N$ Reaction Using Ab Initio $^3A'$ and $^3A''$ Potential Energy Surfaces, *Journal of Chemical Physics*, **104**, (8), pp. 2825-2833, 1996.
18. R. D. Levine and R. B. Bernstein, Molecular Reaction Dynamics and Chemical Reactivity, Oxford University Press, 1987.
19. H. S. Johnston, "Gas Phase Reaction Kinetics of Neutral Oxygen Species", NSRDS-NBS 20, 1968.
20. M. Ju. Pogosbekian, A. L. Sergievskaya, and S. A. Losev, "Verification of Theoretical models of Chemical Exchange Reactions on the Basis of Quasi-Classical Trajectory Calculations", *Chemical Physics*, **328**, pp. 371-378, 2006.
21. M. Capitelli, F. Esposito, E. V. Kustova, and E. A. Nagnibeda, "Rate Coefficients for the Reactions N2(i)+N=3N: A Comparison of Trajectory Calculations and the Treanor-Marrone Model", *Chemical Physics Letters*, **330**, pp. 207-211, 2000.
22. A. L. Sergievskaya, E. A. Kovach, S. A. Losev, and N. M. Kuznetsov, "Thermal Nonequilibrium Models for Dissociation and Chemical Exchange Reactions at High Temperatures", AIAA Paper 96-1895, American Institute of Aeronautics and Astronautics, Reston, VA, 1996.